Research on predictive current control method of PMSM for continuous switched boost inverter

IOP Conf. Series: Materials Science and Engineering **533** (2019) 012005 doi:10.1088/1757-899X/533/1/012005

Research on predictive current control method of PMSM for continuous switched boost inverter

Liyong Yang, Shuo Han, Shuo Liu and Xiaojuan He

College of Electrical and Control Engineering in North China University of Technology, Beijing 100144, China

hanshuo930204@163.com

Abstract. In this paper, the continuous switched boost inverter (CSBI) is used to improve permanent magnet synchronous motor (PMSM) control performance through predictive control, aiming at the drawback of the traditional PMSM drive system. Between the inverted circuit and the input DC power, a switched boost circuit is added to form a switched boost inverter circuit to achieve higher voltage gain and eliminate the dead band. Meanwhile, the drive system has higher reliability. Moreover, the paper adopts predictive current control (PCC) to control PMSM, comparing with the traditional field oriented control (FOC), PCC has faster dynamic performance and reduces current ripple. Finally, the simulation and experimental results verify the feasibility of the based on the continuous switched boost inverter of predictive current control for PMSM.

1. Introduction

Permanent magnet synchronous motor (PMSM) has high efficiency and power factor comparing with direct current machines and induction machines. It possesses characteristics such as less heat, small, simple structure, large overload current and high reliability. It has been widely used in industrial and agricultural production, industrial automation and information technology field [1]. The traditional drive system modulation usually adopts the space vector pulse width modulation (SVPWM) [2], which can reduce harmonic distortion. Meanwhile, SVPWM technology with the continuous switched boost inverter (CSBI) has good ability to resist electromagnetic interference (EMI) and avoids the distortion of the output waveform [3].

CSBI has high boost capability and shoot-through immunity, it combines the high gain of Z-source inverter

(ZSI) [4] and switched boost inverter (SBI) [5] characteristics using a small number of passive components. The CSBI has only one LC filter from the inverter structure. Meanwhile, based on continuous switched boost inverter, establishing the relationship of DC input and alternating current (AC) output analyzes steady state of the inverter.

PMSM control methods are proposed to have good dynamic response performance, such as adaptive PID controller [6], neuro-fuzzy controller [7], direct predictive control (DPC) [8], dead-beat PC [3]. These control schemes have different defects which include fast response, torque ripple, system delay, uncertain parameters and so on. However, predictive current control (PCC) combines advantages of DPC and deadbeat PC, and has been applied successfully in PMSM control.

The cost function is chosen appropriately to force the control process to reach the desired standard for PCC method. It contains the current control squared error, and also adds additional conditions to the controller to satisfy the implementation of several additional criteria. The PCC optimizes the voltage vector and the duty cycle to the cost function which guarantees the global optimum of the selected voltage vector, and obviously improves the steady-state performance of the system.

2. Continuous switched boost inverter

2.1. CSBI topology

CSBI gets high gain and can improve EMI immunity in the boost mode. The inverter combines the advantages of the traditional voltage source inverter (VSI) [5], the SBI and the ZSI. It has the same gain as the ZSI, and possesses the same number of components as the SBI. It doesn't need the dead band of the switch signals, so the output waveform distortion could be avoided [5]. The topology of CSBI with the PMSM as shown in Fig. 1.

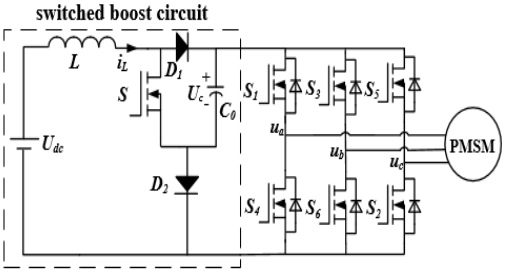

Figure 1. Topology of CSBI

2.2. CSBI operation

The CSBI can provide high voltage gain and can work in two states: shoot-through state and non-shoot-through state. In the shoot-through state, the inductor L is charged by capacitor C_0 and input power U_{dc}. In the non-shoot-through state, the capacitor C_0 is charged by the inductor L. The equivalent circuits of the CSBI in the shoot-through and non-shoot-through state are shown in Fig. 2.

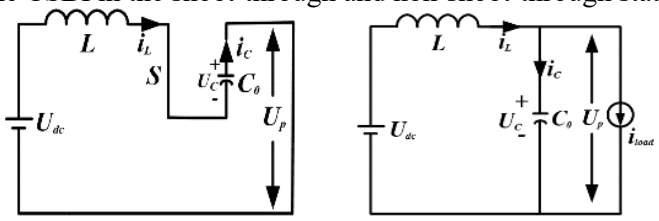

Figure 2. Equivalent circuit of the CSBI: (a) shoot-through state and (b) non-shoot-through state

When the inverter operates in the shoot-through state, the voltage of inductor L and the current of capacitor C_0 are given by Fig.2(a).

$$\begin{cases} U_L = U_{dc} + U_C \\ i_C = -i_L \end{cases} \tag{1}$$

When the inverter operates in the non-shoot-through state, the voltage of inductor L and the current of capacitor C_0 are given by Fig.2(b).

$$\begin{cases} U_L = U_{dc} - U_C \\ i_C = i_L - i_{load} \end{cases} \tag{2}$$

where U_L is the voltage of the inductor L; U_{dc} is the input source; U_C is the voltage of the capacitor C_0; i_L is the current of the inductor L; i_C is the current of the capacitor C_0, and i_{load} is the output current of the inverter.

When the steady state equilibrium, using the volt-second balance of inductance and the

amp-second balance of capacitor can get the voltage conversion ratio *B* of the CSBI [9],

$$B=\frac{U_C}{U_{dc}}=\frac{1}{1-2D} \tag{3}$$

Where *D* is the shoot-through duty cycle, and *B* is the voltage conversion ratio of CSBI. The relationship between voltage conversion ratio and shoot-through duty cycle is shown in Figure 3. Fig. 3 can be seen the *B* of the system increases with the increase of *D*.

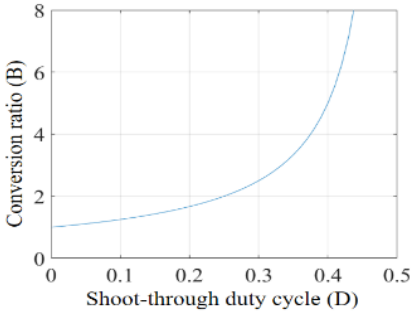

Figure 3. Relationship between voltage conversion ratio and shoot-through duty ratio

3. PMSM model and control strategy

PCC [6] aims to improve the response speed and steady-state error of PMSM, and the PCC replaces the PI controller to use current control in the FOC. Similar to other predictive control methods, the PCC based on the motor model in the switching period to get the desired current, the feedback of the desired currents are i_{dk} and i_{qk}, the value of rotor speed ω_s from coder and the value of the *d-q* currents. Fig.4 shows the diagram of the PCC algorithm using a PI controller as a speed control loop. This paper uses i^*_{dk}=0 control method.

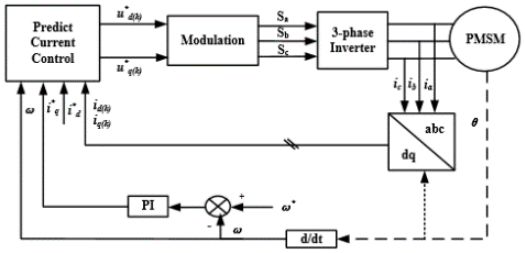

Figure 4. Block diagram of the PCC algorithm

3.1 Discrete model of PMSM

In the PCC algorithm [6], the control variables are stator currents. In order to predict the stator currents of given switching states, the differential equation model needs to transform to discrete time model based on the dynamic model of the motor. In this way, the next state of *d-q* currents is predicted by the current value of the *d-q* currents, the measured electrical angle and the input *d-q* voltages. When the sampling period is very short, the surface mounted PMSM ($L=L_d=L_q$) is created a discrete time model by Taylor series expansion [6].

$$\begin{cases} i_{dk+1}=(1-\dfrac{RT_s}{L_d})i_{dk}+\omega_{sk}T_s i_{qk})+\dfrac{T_s}{L_d}u_{dk} \\ i_{qk+1}=(1-\dfrac{RT_s}{L_q})i_{qk}-\omega_{sk}(T_s i_{dk}+\dfrac{T_s\psi_f}{L_q})+\dfrac{T_s}{L_q}u_{qk} \end{cases} \tag{4}$$

3.2 Predictive Current Control Method

The design of the controller involves the calculation of the reference voltage that should be implemented in the current time step, so as to ensure that the current will follow the reference voltage in the next step. This goal is to get the minimum value of the difference between the predicted currents i_{dk+1}, i_{qk+1} and the reference values i^*_{dk}, i^*_{qk}.

The cost function selects the voltage vector that minimizes between the predicted current and given current. It contains the current control squared error, and adds additional conditions to the controller to satisfy the implementation of several additional criteria. The value of predictive current can be given by the discrete model (4) of PMSM, a cost function [7] is calculated as follows:

$$g(u^*_{dk}, u^*_{qk}) = i_{dk+1}{}^2 + (i_{qk+1} - i^*_{qk})^2 \tag{5}$$

The cost function includes u^*_{dk} and u^*_{qk}, it must ensure that achieves the minimum value in each step. Through (4), the predictive currents i_{dk+1}, i_{qk+1} can be expressed the reference voltages u^*_{dk}, u^*_{qk}, and measured currents i_{dk}, i_{qk}, and speed value ω_s, respectively.

The cost function is rewritten as,

$$g(\mathbf{u}_k) = \mathbf{u}_k^T \lambda^2 \mathbf{u}_k + \mu_k \mathbf{u}_k \tag{6}$$

The parameters of this cost function are defined as:

$$\mathbf{u}_k = \begin{bmatrix} u_{dk} \\ u_{qk} \end{bmatrix}$$

$$\lambda = \frac{T_s}{L_{dq}}$$

$$\mu_{1k} = 2\lambda\left(i_{dk} - \frac{RT_s}{L_{dq}} i_{dk} + \omega_{sk} T_s i_{qk+1}\right)$$

$$\mu_{2k} = 2\lambda\left(-\omega_{sk} T_s i_{dk} + i_{qk} + \frac{RT_s}{L_{dq}} i_{qk} - i^*_{qk} - \omega_{sk} \frac{T_s}{L_{dq}} \psi_f\right)$$

$$\mu_k = [\,\mu_{1k} \quad \mu_{2k}\,]$$

The diagonal-constant matrix $\boldsymbol{\mu}_k$ of ĝ is time variable, because they depend on the feedback currents i_{dk}, i_{qk} and rotor speed ω_{sk}. Moreover, $\boldsymbol{\mu}_{2k}$ depends on the output of the speed control loop orthogonal reference current i^*_{qk}. Therefore, the optimization process takes place at each time step and produces a variable voltage reference signal.

Because of the safety and reliability of the motor, an additional constraint is required that the current amplitude does not exceed a certain maximum value. The technical specifications of the motor select the maximum current as the maximum transient permissible current.

The maximum current constraint needs a certain limit; that is,

$$\begin{cases} i_{dk+1} < i_{MAX} \\ i_{qk+1} < i_{MAX} \end{cases} \tag{7}$$

Substitute (4) into (7) to obtain the optimal voltage value for the controller,

$$\begin{cases} u^*_{dk} < \dfrac{1}{\lambda}\left(i_{MAX} - i_{dk} + \dfrac{RT_s}{L_{dq}} i_{dk} - \omega_{sk} T_s i_{qk}\right) \\ u^*_{qk} < \dfrac{1}{\lambda}\left(i_{MAX} + \omega_{sk} T_s i_{dk} - i_{qk} + \dfrac{RT_s}{L_{dq}} i_{qk}\right) + \omega_{sk} \psi_f \end{cases} \tag{8}$$

By using the Newton's iterative optimal algorithm, the system can run the optimization process, and the r+1 iteration function is expressed by the function of the rth iteration result [6], that is,

$$\mathbf{u}_{kr+1} = \mathbf{u}_{kr} - \gamma\left(\mathbf{u}_{kr} + \frac{1}{2\lambda^2} \mu_K^T\right) \tag{9}$$

The coefficient γ ($0<\gamma<1$) of the Newton's method is introduced to modify. It can reduce the step size to prevent potential numerical instability, divergence, and overshooting.

Table 1. Parameter of the used PMSM

Parameter	Value
Rated Voltage U_n	160V
Rated Current I_n	5.5A
Rated Speed ω_n	1200r/min
Inductance L	17mH
Per Phase Winding Resistance R	1.3Ω
Torque Constant k_m	1.23Nm/A
Number of Pole Pairs n_p	3
Inertia J	0.00087kg·m^2

Table 2. Parameters of the control system

Parameter	Value
Switching frequency f_s	5kHz
Sample time T_c	0.2μs
Boost circuit inductance L	2mH
DC bus capacitor bank C_0	560μF
Optimization step coefficient γ	0.7

4. Simulation results

In this part, Fig. 5 shows the relationship between the input voltage U_{dc} and the bus voltage U_c. Then, the PCC algorithm in SVPWM was carried out using a PMSM. Nominal parameters are given in Table 1, and the performance of the PCC scheme has been analyzed by simulation. Table 2 shows the parameters of the Control System, and the shoot-through duty cycle is D=0.2 in this simulation.

4.1. The input voltage and the bus voltage simulation results of CSBI

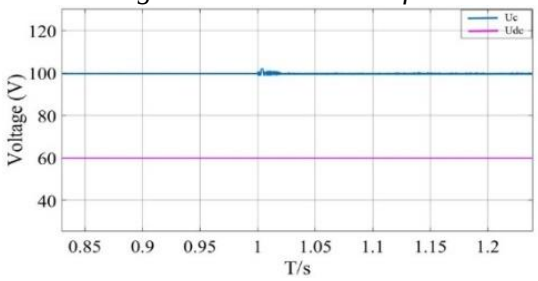

Figure 5. The input voltage and the bus voltage

In Fig.5, the input voltage U_{dc} is 60V, according to (3) gets the bus voltage U_c after boost circuit. The steady state after external load, the bus voltage is 100V satisfying the equation (3).

4.2. PMSM simulation results

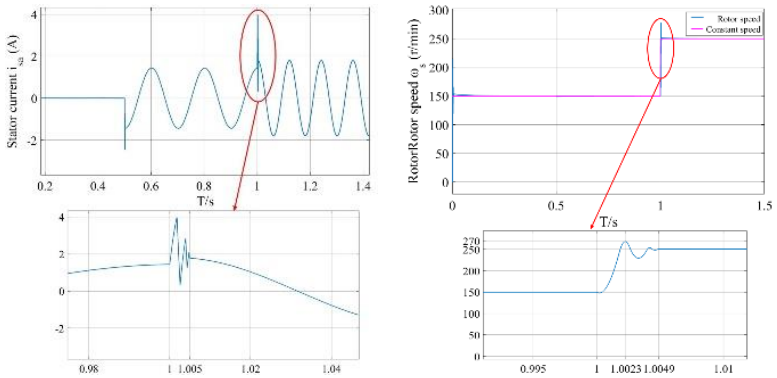

(a) (b)

Figure 6. Simulation results: (a) stator current waveform and (b) rotor speed waveform

The motor starts at no-load. Then, a step of external load is 0.2 N· m and a constant speed is about 150r/min that are applied at about t=0.5s and then removed at t=1s. Finally, a step of external load is 0.5 N· m and a constant speed is about 250r/min that are applied at about t=1s and then removed at t=1.5s.

In Fig.6(a), after external load, the waveform of the stator current could recover quickly. In Fig.6(b), under the SVPWM, the PCC peak time is 0.0023s, the maximum speed overshoot is 8%, and the transient time is 0.0049s.

The performance of the PCC has been analyzed by simulation results as shown in the Table 3.

Table 3. Simulation Results for PCC.

	PCC
Speed peak time	0.0023s
Speed transient time	0.0049s
Speed overshoot	8%
Speed steady-state error	0

5. Experimental results

The experimental setup basically consisted of a PMSM with a control board implemented in stm32f407ZGT6 and EMP570T100C5. Then, it verifies the relationship between the input voltage U_{dc} and the bus voltage U_c. The PMSM and the control system parameters are the same as Table 1 and Table 2, and the shoot-through duty cycle is D=0.3 in this experiment.

5.1. The input voltage and the bus voltage experimental results of CSBI

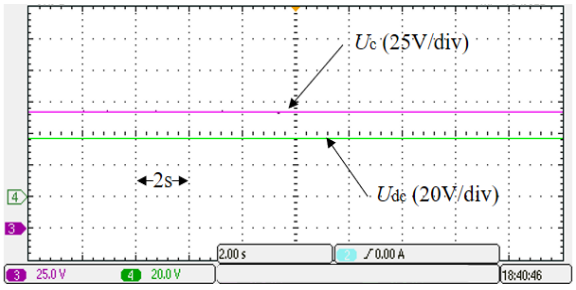

Figure 7. The input voltage and the bus voltage (2s/div)

In Fig.7, the input voltage U_{dc} is 36V, according to the equation (3) gets the bus voltage U_c after boost circuit. The bus voltage is 92.5V satisfying the equation (3) after the steady state.

5.2. PCC experimental result

In this part, the motor starts at no-load. Then, a constant speed is 50r/min, and a constant speed changes 200r/min a few minutes later.

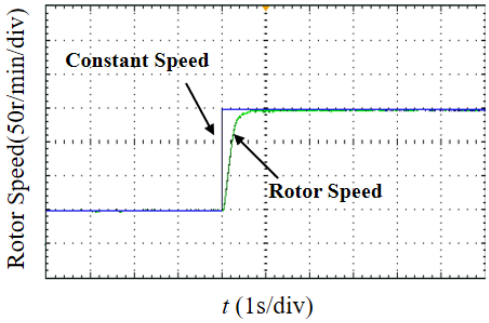

Figure 8. Rotor speed experimental results (1s/div)

Fig.8 shows the rotor speed experimental results of a speed controller with the PCC method. The speed rising time is 0.8s. Meanwhile, the PCC method has not overshoot and steady-state error. The PCC algorithm possesses preferable response speed.

6. Conclusion

This paper designs a kind of PCC of PMSM for the CSBI, it combines and improves the CSBI, SVPWM method and PCC algorithm. The PMSM drive system can obtain the continuous input current from DC power source, and avoid the output waveform distortion. When the input voltage fluctuation, the voltage of the capacitor remains the same. It can be seen from the simulation and experimental results that the same results can be obtained by using the PCC method based on the CSBI. Meanwhile, the control system also acquired excellently steady control effect.

References

[1] Alacoque J C. Direct Eigen Control for Induction Machines and Synchronous Motors[M]. Wiley & Sons, 2013.
[2] Singh S, Tiwari A N. Analysis and Simulation of Vector Controlled PMSM Drive using SVPWM Inverter[C]. International Conference for Convergence in Technology. 2017.
[3] Zhang X, Hou B, Mei Y. Deadbeat Predictive Current Control of Permanent-Magnet Synchronous Motors with Stator Current and Disturbance Observer[J]. IEEE Transactions on Power Electronics, 2017, 32(5):3818-3834.
[4] Yu K, Xiong B, Zhao J. A comprehensive study of space vector pulse-width modulation technique for three-phase Z-source inverters[J]. International Journal of Circuit Theory & Applications, 2016, 44(2):364-381.
[5] Meinagh F A A, Babaei E, Tarzamni H. Modified high voltage gain switched boost inverter[J]. Iet Power Electronics, 2017, 10(13):1655-1664.
[6] Alexandrou A D, Adamopoulos N K, Kladas A G. Development of a Constant Switching Frequency Deadbeat Predictive Control Technique for Field-Oriented Synchronous Permanent-Magnet Motor Drive[J]. IEEE Transactions on Industrial Electronics, 2016, 63(8):5167-5175.
[7] Bozorgi A M, Farasat M, Jafarishiadeh S. Model predictive current control of surface-mounted permanent magnet synchronous motor with low torque and current ripple[J]. Iet Power Electronics, 2017, 10(10):1120-1128.
[8] Antonello R, Carraro M, Peretti L, et al. Hierarchical Scaled-States Direct Predictive Control of Synchronous Reluctance Motor Drives[J]. IEEE Transactions on Industrial Electronics, 2016, 63(8):5176-5185.
[9] Nag S S, Mishra S. Current-Fed Switched Inverter[J]. IEEE Transactions on Industrial Electronics, 2014, 61(9):4680-4690.